Constraints on T_c for superconductivity in heavily boron-doped diamond

Jonathan E. Moussa* and Marvin L. Cohen

Department of Physics and Materials Sciences Division, Lawrence Berkeley National Laboratory, University of California at Berkeley, Berkeley, California 94720, USA

(Received 27 November 2007; revised manuscript received 25 January 2008; published 27 February 2008)

Calculations of electron-phonon coupling are performed for boron-doped diamond structures without electronically compensating defects over a wide range of boron concentration. The effects of boron substitutional disorder are incorporated through the use of randomly generated supercells, leading to a disorder-broadened distribution of results. After averaging over disorder, this study predicts a maximum bulk T_c near 55 K for boron concentrations between 20% and 30%, assuming the validity of the simple structural model used and a Coulomb pseudopotential of $\mu^*=0.12$. Considering only the largest electron-phonon coupling values of the distribution, superconductivity may still percolate through the material at higher temperatures, up to 80 K, through the regions of large coupling. A synthesis path is proposed to experimentally access this class of materials.

DOI: 10.1103/PhysRevB.77.064518 PACS number(s): 74.62.Bf, 74.62.Dh, 74.70.Ad

I. INTRODUCTION

The theory of phonon-mediated conventional superconductivity is now established well enough to be used to predict properties of superconductors before they are synthesized. A notable success of this approach was in predicting the transition temperatures of a series of high-pressure metallic phases of silicon.[1] More typical are predictions that remain unfulfilled, such as a predicted[2] T_c of 29 K in MoN or more recent predictions[3] of superconductivity in hole-doped LiBC. The difference between these successful and unverified predictions is that the high-pressure phases of silicon have well-characterized simple unit cells that agree with theory, while the predicted MoN and hole-doped LiBC structures are theoretical assumptions that have not been experimentally realized due to unforeseen structural defects.[4,5] This highlights the need to study the normal state material aspects of hypothetical superconductors just as carefully as superconducting properties for such predictions.

In this paper, we study boron-doped diamond, a recently discovered class of superconductors for which the transition temperature has steadily risen due to advances in material synthesis and increased boron concentrations from an initial value[6] of 4 K to the current best value[7] of 11 K. In the presently accessible doping regime of up to 6% boron concentration, T_c is observed to rise steadily and monotonically with substitutional boron concentration provided that there is no significant concentration of compensating defects.[8] In order to motivate the synthesis of even more heavily doped diamond, we calculate a predicted T_c versus boron concentration curve that extends to 50% doping, going well beyond what is likely to be the experimentally accessible doping regime. This prediction is based on a simple model of boron disorder in diamond and a neglect of defects other than substitutional boron. Based on recent reports[9] of incorporation of up to 38% boron in diamond, we propose a synthesis path to materials that may coincide with this model and attain T_c values as high as 55–80 K.

The results we obtain for boron-doped diamond are similar to predictions[10] made for $Li_{1-x}BC$, since both materials derive their strong electron-phonon coupling from B-C bonding states.[11] An important difference between the sp^2 bonded planes of $Li_{1-x}BC$ and sp^3 bonded framework of boron-doped diamond is their sensitivity to disorder. Lithium removal induces B-C disorder in the graphitic BC plane of $Li_{1-x}BC$, pushing the strongly electron-phonon coupled σ states below the weakly coupled π states and away from the Fermi level.[5] In boron-doped diamond, all valence states are σ states with strong electron-phonon coupling, and the only scenario in which substitutional disorder can quench superconductivity is if it is strong enough to open up a gap in the valence states.

There has been recent progress on improving the accuracy and efficiency of electron-phonon coupling calculations, in practically including electron anisotropy and phonon anharmonicity[12] and in using Wannier functions to perform Fermi surface integrals to high precision.[13] However, the case of heavily boron-doped diamond provides a new challenge of strong disorder, where there is not a single unique structure that can be carefully studied with accurate methods. The coherent potential approximation has recently been used to study disorder in boron-doped diamond[14,15] but is presently unable to account for the effects of structural relaxation that become important at high boron concentrations. Anderson's prescription[16] for dealing with strong disorder is to perform a calculation on the entire nonperiodic material or some finite representation thereof, representing Cooper pairs as time-reversed pairs of disordered electron eigenstates rather than periodic Bloch states. With modern computational resources, it is not possible to use a large enough unit cell to converge with respect to disorder. This limitation can be bypassed by approximating the disordered material with a statistical sampling over a set of smaller disordered unit cells. This necessitates the calculation of electron-phonon coupling for a large number of systems with less stringent requirements of precision since the results will be averaged over many calculations and insufficient sampling will be the dominant source of error. Neither electron anisotropy nor phonon anharmonicity are considered in this study. The cost of calculating the isotropic Eliashberg spectral function is significantly reduced by making a Γ-point phonon approxi-

mation and using only diagonal electron-phonon matrix elements. These approximations are shown to be valid for the boron-doped diamond structures studied.

II. COMPUTATIONAL METHODOLOGY

The state of the art assumptions associated with calculations of electrons in solids are made here, that the normal state of the electrons is described by density functional theory (DFT) and that the properties of the superconducting state can be related to normal state properties through the Migdal–Eliashberg theory.[17] More specifically, the PWSCF[18] and SIESTA[19] computer programs are utilized to perform DFT calculations within a plane-wave and local-orbital basis set, respectively. All structures are relaxed within a variable unit cell to their theoretical equilibrium configurations before electron-phonon properties are calculated. Electron-phonon properties are calculated using a frozen-phonon approximation considering only Γ-point phonons. This limited set of electron-phonon properties is sufficient to construct a novel approximation to the isotropic Eliashberg spectral function, derived below, that adequately describes the boron-doped diamond structures studied in this paper. For an N-atom unit cell, all the required phonon and electron-phonon properties are obtained from electronic band energies and atomic forces of $3N+1$ ground state calculations—of the base structure and of perturbations of each atom in each of the three Cartesian directions, from which finite-difference derivatives are calculated. The phonon calculations require second derivatives of total energy with respect to atomic coordinates, which are equivalent to the first derivatives of the atomic forces, $d^2E/d\mathbf{R}_i d\mathbf{R}_j = -d\mathbf{F}_i/d\mathbf{R}_j$. These derivatives, along with the atomic masses M_i, are used to calculate the Γ-point phonon frequencies ω_m^0 and lattice displacement vectors ξ_m^0, using the dynamical matrix eigenvalue equation

$$M_i(\omega_m^0)^2[\xi_m^0]_i = \sum_{j=1}^{N} \frac{d^2E}{d\mathbf{R}_i d\mathbf{R}_j} \cdot [\xi_m^0]_j, \tag{1}$$

where $[\cdots]_i$ denotes real-space vectors indexed over atoms in the unit cell and ξ_m^0 are normalized to 1. Correspondingly, only the diagonal electron-phonon matrix elements associated with electrons interacting with the Γ-point phonons are calculated. These matrix elements are simply the perturbations of the electronic band energies with respect to phonon displacements and can be calculated as perturbations with respect to atomic displacements,

$$\langle n\mathbf{k}|\frac{dV_{SCF}}{d\mathbf{R}_i}|n\mathbf{k}\rangle = \frac{d\epsilon_{n\mathbf{k}}}{d\mathbf{R}_i}, \tag{2}$$

and then transformed to phonon coordinates. These are deformation potentials and have been used previously to estimate the electron-phonon coupling in boron-doped diamond.[20]

Like most conventional superconductors, boron-doped diamond is believed to have a sufficiently isotropic gap function such that it is well described by the isotropic Eliashberg spectral function defined as

$$\alpha^2F(\omega) = N_\uparrow(\epsilon_F)^{-1} \sum_{m,n\mathbf{k},n'\mathbf{k}'} |g^m_{n\mathbf{k},n'\mathbf{k}'}|^2 \times \delta(\epsilon_F - \epsilon_{n\mathbf{k}})\delta(\epsilon_F - \epsilon_{n'\mathbf{k}'})\delta(\omega - \omega_m^{\mathbf{k}-\mathbf{k}'}), \tag{3}$$

where $N_\uparrow(\epsilon_F)$ is the density of states per spin at the Fermi level, the sum is over all phonon branches and all electronic states excluding spin degeneracy, and $g^m_{n\mathbf{k},n'\mathbf{k}'}$ is the electron-phonon matrix element,

$$g^m_{n\mathbf{k},n'\mathbf{k}'} = \sum_i \frac{[\xi_m^{\mathbf{k}-\mathbf{k}'}]_i}{\sqrt{2M_i\omega_m^{\mathbf{k}-\mathbf{k}'}}} \cdot \langle n\mathbf{k}|\frac{dV_{SCF}}{d\mathbf{R}_i}|n'\mathbf{k}'\rangle. \tag{4}$$

In this study, an approximate Eliashberg spectral function requiring only Γ-point phonon frequencies and diagonal electron-phonon matrix elements,

$$\alpha^2F_\Gamma(\omega) \equiv \sum_{m,n\mathbf{k}} |g^m_{n\mathbf{k},n\mathbf{k}}|^2 \delta(\epsilon_F - \epsilon_{n\mathbf{k}})\delta(\omega - \omega_m^0), \tag{5}$$

is used in place of $\alpha^2F(\omega)$. The form of $\alpha^2F_\Gamma(\omega)$ is derived from Eq. (3) by approximating that the electron-phonon matrix elements are isotropic, $g^m_{n\mathbf{k},n'\mathbf{k}'} \approx g^m_{n\mathbf{k},n\mathbf{k}}$, and that the phonon bands are flat, $\omega_m^{\mathbf{k}-\mathbf{k}'} \approx \omega_m^0$. The flat phonon band approximation can be systematically improved by increasing the size of the unit cell, which shrinks the volume of the Brillouin zone and reduces the dispersion of phonon bands. Convergence with respect to unit cell size is examined in Sec. III.

Disorder in the boron-doped diamond system is approximated by the random substitution of boron atoms into a supercell of the diamond lattice. This leads to large, nonsymmetric unit cells that necessitate limitations on the calculations performed. We use SIESTA instead of PWSCF to calculate electron-phonon and dynamical matrix elements, a significant computational saving that leads to errors of a few percent from the PWSCF values. For the electronic calculations, the Brillouin zone is sampled using a standard uniform grid of k points and converged with respect to a 0.3 eV Gaussian smearing. Equation (5) is a weighted electronic density of states at ϵ_F and converges as $N(\epsilon_F)$ does with respect to electronic $\mathbf{k}$-point sampling and δ-function smearing. The smearing is physically justified in diamond due to electronic spectral broadening of several tenths of an eV caused by boron substitutional disorder for concentrations as small as 2.5% boron.[14]

The generalized Allen–Dynes formula[21] is used to calculate T_c because of its ability to interpolate between the weak-coupling limit, $T_c \sim \omega_{ph}\exp[-(1+\lambda)/\lambda]$, and strong-coupling limit, $T_c \sim \omega_{ph}\sqrt{\lambda}$. Averaged phonon frequencies and λ are calculated using $\alpha^2F_\Gamma(\omega)$ in place of $\alpha^2F(\omega)$. For T_c calculations, the Coulomb pseudopotential μ^* is given a standard value of 0.12. Disorder can enhance the value of μ^* through localization effects,[22] but calculations of such corrections are beyond the scope of this paper. The μ^* enhancement is known to be significant when the Fermi level is in the vicinity of a mobility edge. In heavily boron-doped diamond, the

Fermi level is deep within the valence band and presumably away from a mobility edge, which should result in a negligible μ^* enhancement.

III. SUPERCONDUCTIVITY IN HEAVILY BORON-DOPED DIAMOND

Boron is incorporated into the diamond lattice, through both equilibrium[6] and nonequilibrium[9] methods, without any observed ordering. The introduction of disorder would not have a strong effect on dilute impurities that are too distant to interact, but in the limit of very large boron concentration, disorder may play an important role in the superconductivity of the material. At high enough boron concentrations, heavily boron-doped diamond eventually enters the regime of the dirty superconductor, as described by Anderson who prescribes[16] directly diagonalizing the electronic states of the impure crystal rather than considering the scattering of Bloch states off impurities. The Cooper pairs of the superconducting state are then comprised of time-reversed pairs of electron eigenstates of the impure crystal rather than Bloch states of the conventional unit cell of the pure crystal. In order to approximate a disordered crystal of heavily boron-doped diamond, we consider periodic crystals with unit cells that are supercells of the primitive unit cell of diamond randomly modified according to a structural model of the disorder present in the material. Because these supercells will not be large enough to accurately represent the disordered boron-doped diamond material by themselves, each randomly generated structure will have a significantly different Eliashberg spectral function. This variation is representative of the local variations in electron-phonon coupling possible in the impure crystal. The superconducting coherence length diverges at the transition temperature, which suggests that T_c for bulk superconductivity should be well described by a spectral function averaged over the ensemble of random structures that only has a dependence on the average boron concentration. At temperatures higher than the bulk T_c, there may still be superconductivity in regions of the crystal where local variations lead to a larger than average electron-phonon coupling. Whether this leads to a superconducting state that percolates through the crystal or a granular superconductor is beyond the scope of this paper.

The majority consensus on the mechanism for superconductivity in boron-doped diamond is that substitutional boron acts as a shallow acceptor in diamond that is incorporated into the valence band as a hole.[14,23] At low boron concentrations, substitutional boron can form dimers and become deeper acceptors that do not donate holes to the valence band, but at concentrations greater than 3% boron, even these complexes donate holes.[24] More detailed theoretical studies of boron-based defects in diamond[25] show that all studied substitutional boron complexes act as acceptors, while complexes containing vacancies or interstitials typically act as donors. Donor impurities passivate the holes in the valence band, reducing the electronically active boron concentration of the material. Particularly detrimental are interstitial boron atoms, which are donors that can passivate up to three holes per boron atom, depending on the local environment around the interstitial.

Hydrogen-based defects are also relevant to the problem of boron-doped diamond superconductivity as chemical vapor deposition (CVD) diamond synthesis takes place in a hydrogen plasma that inadvertently incorporates hydrogen into the synthesized material.[8] Hydrogen in boron-doped diamond typically forms complexes with substitutional boron and even more stable complexes with boron dimers.[26] In all of these cases, every hydrogen atom passivates one hole.

The simplest approach to studying the upper limits of T_c in boron-doped diamond is to study a model of the material that neglects all avoidable detriments to superconductivity. The basic model suggested by the experiment[8] is that T_c is a monotonically increasing function of hole concentration, making compensating donor defects uniformly detrimental to superconductivity. In the absence of compensating defects, T_c should then monotonically increase as a function of substitutional boron concentration. In Sec. IV, we propose a synthesis path that completely avoids hydrogen- and vacancy-based defects and is likely to avoid interstitial boron for some range of boron concentrations. This allows us to rule out these defects in our structural model of boron-doped diamond. The only disorder left for the structural model is the boron substitutional disorder, which is not presently avoidable as there are no experimental reports of diamond- or graphitelike boron-carbon materials with three-dimensional crystalline order. While the details of a synthesis process might favor specific local configurations of boron, such details are not at present known. Because the synthesis will be a nonequilibrium process, total-energy-based criteria for choosing structures also are not physically justified. However, there is a theoretical study of the energetics of boron ordering in graphite[27] that suggests that boron nearest neighbors in graphite are energetically unfavorable. This may be relevant if boron-doped graphite is an intermediate material in the synthesis process. The resulting structural model for boron-doped diamond is assumed to be purely random substitution of boron into the diamond lattice, with an additional constraint based on boron ordering in graphite used for a subset of the calculations.

We perform two complementary sets of calculations over randomly generated boron-doped diamond structures: a large set of small supercell calculations to get a good average over disorder and a small set of large supercell calculations to estimate convergence with respect to supercell size. There is no clear limit to how much substitutional boron can be incorporated into the diamond lattice, but a suitably large upper limit used for this study is 50% boron. The first set of calculations utilizes a 24-atom $2\times2\times3$ supercell of the primitive diamond unit cell and consists of 256 randomly substituted structures relaxed using SIESTA with a double-zeta-polarized basis set. This set of structures includes 1 structure with one boron per cell, 5 inequivalent structures with two borons per cell, and 25 structures each for all higher boron concentrations. The second set of calculations utilizes a 54-atom $3\times3\times3$ supercell of the primitive diamond unit cell with 27 structures, one for each boron concentration, relaxed using PWSCF. The structures of this second set are generated with an additional constraint based on the specific synthesis proposal in Sec. IV. Within the prebuckled graphite precursor to the diamond structure, boron nearest neighbors

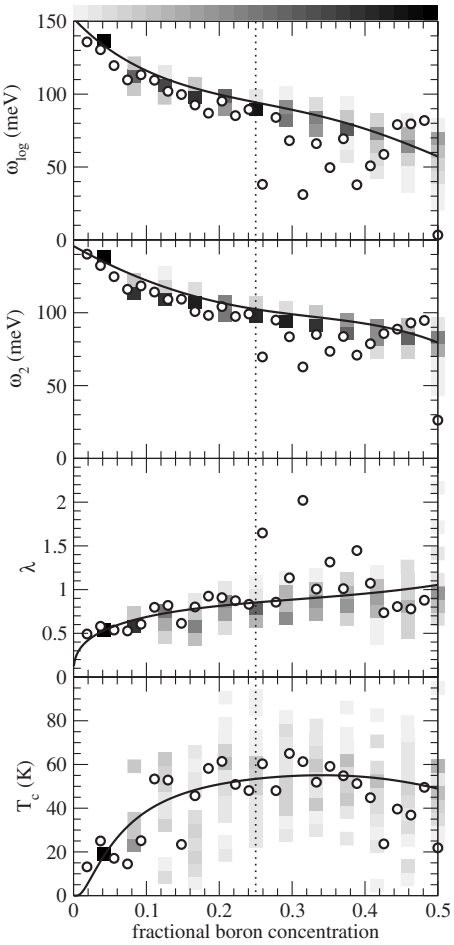

FIG. 1. Average phonon frequencies, coupling constant, and Allen–Dynes formula T_c values for the large (circle) and small (box) supercell calculations and the bulk average (line). The gray-scale values of the boxes represent the fraction of data points at that boron concentration in the interval spanned by the box. An outlier is omitted, $\lambda=7.5$ at 50% boron doping for the large supercell. Boron concentrations beyond 25% are in a region of structural instability for which this study is not sufficiently converged with respect to supercell size.

are forbidden due to the large energy penalty for boron clustering in graphite.[27] This constraint significantly reduces the set of possible structures at larger boron concentrations and thus reduces the sampling error due to the small number of structures considered for the large supercell.

The results of both sets of boron-doped diamond calculations are displayed in Fig. 1. Plotted are the T_c values calculated from the Allen–Dynes formula[21] and the quantities used in the formula: λ, $\omega_{\log} \equiv \exp\langle \ln \omega \rangle$ and $\omega_2 \equiv \sqrt{\langle \omega^2 \rangle}$. Since only three integrals over $\alpha^2 F(\omega)$ are needed to calculate T_c, there is no need to explicitly generate an averaged boron concentration dependent spectral function. Instead, we fit the three relevant quantities that are linear in $\alpha^2 F(\omega)$—λ, $\lambda\langle \omega^2 \rangle$, and $\lambda\langle \ln \omega \rangle$—to functions of boron concentration using a least-squares procedure. Only the small supercell data set is used in the fit due to inadequate sampling of the large variations in the average phonon frequencies of the large supercell. The fitting function is a third-order polynomial times the cubic root function, which is the doping dependence of the electronic density of states near the band edge for parabolic bands in three dimensions. The least-squares fit is weighted by the inverse square root of the number of data points at a given boron concentration to avoid biasing the fit to the high concentration regions that have more data points. A limitation of this fitting procedure is that it assumes that the average boron concentration of the material is equal to the local average in each supercell, ignoring long-range fluctuations in boron concentration.

The averaged T_c values correspond to bulk superconductivity and have a broad plateau near 55 K for boron doping greater than 20%. A superconducting state may still percolate through the material at temperatures higher than the bulk T_c values, their higher T_c being set by an averaged spectral function including only a subset of the material with above-average electron-phonon coupling. The variance in electron-phonon coupling in the data set suggests that there might still be a substantial fraction of the material able to superconduct in the 70 –80 K regime. The data suggest a rapid, exponential increase in T_c for boron doping levels up to around 6%, associated with the weak-coupling limit of superconductivity. Beyond 6% boron doping, the material is in an intermediate-coupling regime, where T_c is less sensitive to variations in λ and has a broad plateau over a wide boron concentration. The strong-coupling bound[21] on T_c at $\mu^*=0.12$, $T_c \leq 0.16\sqrt{\lambda\langle \omega^2 \rangle}$, is plotted in Fig. 2 and has a similar featureless plateau beyond 6% boron doping. There is a factor of 3 difference between the strong-coupling bound and calculated T_c values because λ saturates near a value of 1. Values of λ between 2 and 3 are required to get within 70%–80% of the bound in the case of an Einstein phonon spectrum.

A few structures in the 54-atom supercell data set have λ values much larger than 1, but their T_c values remain similar to the $\lambda \approx 1$ structures. These large λ values are the result of contributions from a small number of very low frequency modes and do not represent the effective λ associated with the higher frequency modes that dominantly contribute to $\lambda\langle \omega^2 \rangle$ and ultimately T_c. Since $\omega_{\log}$ is more sensitive than ω_2 to the low frequency part of the phonon spectrum, the softening of a few phonon modes also causes $\omega_2/\omega_{\log}$ to deviate significantly from 1. In this scenario, the Allen–Dynes formula penalizes the T_c away from the strong-coupling regime through the deviation of $\omega_2/\omega_{\log}$ from 1.[21] The correlation between large $\omega_2/\omega_{\log}-1$ and large λ is apparent in Fig. 1.

In the doping regime up to 25% boron concentration, there appears to be good agreement between the large and small supercells with regard to their phonon frequencies and electron-phonon couplings. This indicates a convergence with respect to supercell size. Beyond 25% boron concentration, the large supercell has a smaller average phonon frequency that is a result of lattice distortions allowed to develop due to an increased number of structural degrees of freedom in the larger unit cell. This effect is unlikely to be converged with respect to supercell size and may lead to qualitatively different behavior at large boron concentrations. We regard the value of 25% doping as the onset of lattice instability and the region beyond is not accurately repre-

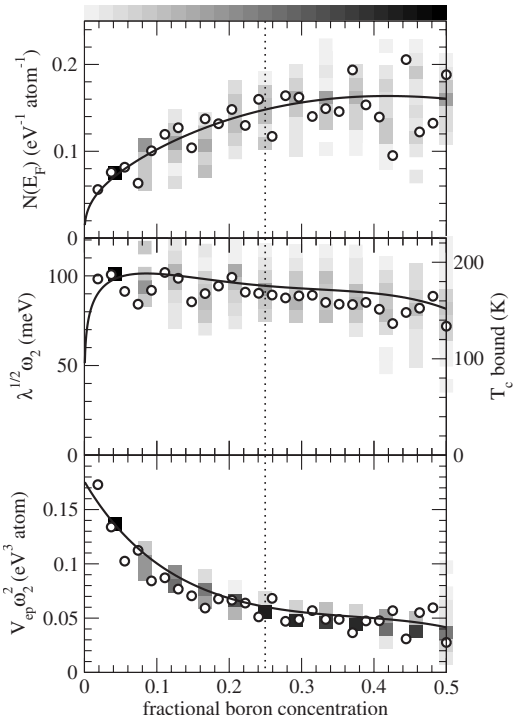

FIG. 2. Density of states and phonon-independent electron-phonon coupling strength for the large (circle) and small (box) supercell calculations and the bulk average (line). The gray-scale values of the boxes represent the fraction of data points at that boron concentration in the interval spanned by the box. Boron concentrations beyond 25% are in a region of structural instability for which this study is not sufficiently converged with respect to supercell size.

sented in this study. If a larger fraction of phonon modes are softened by lattice distortions, both ω_2 and $\omega_{\log}$ may proportionally soften while λ increases, avoiding large values of $\omega_2/\omega_{\log}-1$ that are preventing superconductivity from entering the strong-coupling regime.

Another effect in the unstable region beyond 25% boron doping is an increasing weight at low temperatures in the distribution of T_c values in Fig. 1. The reduced T_c values are caused by an increased weight of reduced $N(\epsilon_F)$ values for doping beyond 25%, as shown in Fig. 2. This can be explained as lattice distortions becoming large enough that they are altering the electronic structure. Chemically, this is due to distortions allowing boron atoms to further fill their $n=2$ electron shell by creating more bonding states. The newly formed bonding (antibonding) states have their energies lowered (raised) from ϵ_F, reducing the number of states at ϵ_F. For larger supercells, this depletion of the Fermi surface may occur at lower boron concentrations and may lead to completely insulating behavior beyond some critical boron concentration.

Lattice distortions at large boron concentration also appear as deviations in the lattice constants from the linear doping dependence expected from Vegard's law,[28] as shown in Fig. 3. The average C-C, B-C, and B-B bond lengths over all studied structures are 1.55, 1.61, and 1.82 Å, which account for the upward deviations in lattice constant due to an increasing number of B-B nearest neighbors at higher boron

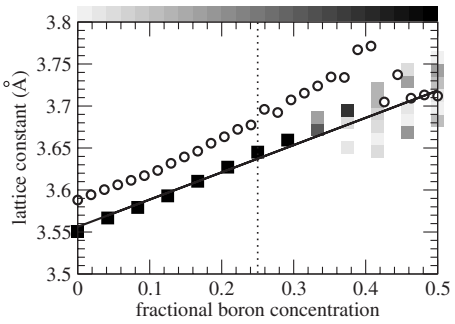

FIG. 3. Lattice constants for the large (circle) and small (box) supercell calculations derived from the volumes of the relaxed supercells. The gray-scale values of the boxes represent the fraction of data points at that boron concentration in the interval spanned by the box. The difference in offset between data sets is within 1% and is caused by their different basis and pseudopotentials. The line is a least-squares fit to the small supercell data set to highlight its deviation from linearity at large boron concentrations.

concentrations. The chemical tendency for boron to form multicenter bonds with other boron atoms can destabilize the diamond structure at higher boron concentrations, causing distortions toward more close-packed, more highly coordinated structures that lead to smaller lattice constants. The measured[9] experimental lattice constant at 38% boron doping is 3.58 Å, which is smaller than the lattice constant calculated in Fig. 3. This deviation suggests that either the experimentally synthesized material is not correctly described by randomly substituted boron or that at this boron concentration the calculations are not converged with respect to supercell size.

Although both $N(\epsilon_F)$ and $\lambda\langle\omega^2\rangle$ are sensitive to disorder through electronic band structure changes, their ratio plotted in Fig. 2 is the least sensitive aspect of electron-phonon coupling observed in this study. The coupling parameter is often decomposed as $\lambda=N(\epsilon_F)V_{ep}$, and the ratio is then $V_{ep}\langle\omega^2\rangle$, independent of $N(\epsilon_F)$. This ratio characterizes the average sensitivity of states at ϵ_F to atomic perturbations without including electron or phonon band structure details.[29] For bonding states in diamond, this sensitivity is determined by the local physics of electronic bonding energies changing with bond length. Such a local property is insensitive to the substitutional disorder in heavily boron-doped diamond.

IV. POSSIBLE SYNTHESIS ROUTES TO HEAVILY BORON-DOPED DIAMOND

To experimentally realize the theoretically possible increase in superconducting transition temperature, as described in Sec. III, it is necessary to synthesize boron-doped diamond with larger concentrations of substitutional boron while keeping sufficiently low the concentration of compensating defects such as vacancies, interstitial boron, and hydrogen. The two main approaches presently used to synthesizing superconducting boron-doped diamond are by placing boron and carbon containing materials under high-pressure and high-temperature conditions[6] or by incorporating boron into the diamond lattice during the CVD of diamond.[7] The

high-pressure, high-temperature approach is an equilibrium process that is ultimately limited by the enthalpy-driven phase separation of boron-carbon compounds[30] into a boron-rich icosahedral boron carbide phase and carbon-rich boron-doped diamond phase with 2% boron concentration, the solubility limit of boron in diamond. CVD growth of diamond is a nonequilibrium process and can go beyond the solubility limit of boron with no clear limitations. The highest T_c that has yet been achieved in CVD diamond is an 11 K onset at 5% boron concentration from growth in the (111) direction,[7] half the predicted value in Fig. 1. The (100) growth direction is able to incorporate even more total boron,[7] up to 10%. However, the (100) growth direction also incorporates a significant concentration of hydrogen into the lattice,[8] compensating much of the boron and presently limiting the T_c to 6 K, far from the prediction based on uncompensated substitutional boron. Continued research on CVD growth of heavily boron-doped diamond may lead to an increase in the substitutional boron concentration and reduction in hydrogen concentration and eventually higher T_c values.

There is a third approach to synthesizing heavily boron-doped diamond that has yet to be considered in the context of superconductivity. High-pressure treatment of a boron-carbon graphitic precursor material at carefully controlled temperatures has been shown[9] to produce boron-carbon systems that by all indications have an sp^3 diamond structure. The graphitic precursors are synthesized using CVD,[31,32] distinct from the diamond CVD process in that the growth does not take place in a hydrogen atmosphere. Because of the absence of a hydrogen atmosphere, hydrogen is not significantly incorporated into the boron-carbon graphite. The main advantage over diamond CVD is that boron has been reported to be incorporated into graphite at concentrations up to 50%,[33] although careful experimental characterization[32] suggests that there is a temperature-dependent limit to substitutional boron concentration beyond which boron is incorporated interstitially. The synthesized graphite has no orientational order between graphitic sheets, but recent results[34] support the existence of pressure-induced direct graphite to diamond transitions in such disordered systems. These results show that covalent bonds are not broken during this transition, preventing new interstitial defects from forming but likely preserving any already-formed interstitial defects of the graphitic precursor. High concentrations of vacancies have not been reported in boron-carbon diamond or graphite structures. As long as the graphitic precursors are synthesized without a large concentration of interstitial atoms, experimental evidence suggests that this approach can lead to boron-doped diamond with a large concentration, 25% or more, of uncompensated substitutional boron.

An added benefit of boron substitution into graphite is a reduction in the pressure required for a direct graphite to diamond transition to occur. This can be interpreted as substitutional boron introduces holes into the π bands of graphite, reducing the structural stability of the flat sp^2 plane. For rhombohedrally stacked graphite, the transition is predicted[35] to occur at 80 GPa. For ordered graphitic BC_3, the transition is predicted[36] to be reduced to 35 GPa. An extreme case is the rhombohedrally stacked graphitic BC with a BN-like in plane ordering, where each boron atom is aligned with a carbon atom in a neighboring plane. We calculate that this material spontaneously buckles into a diamond structure at zero pressure and requires 15 GPa of negative pressure to stabilize the graphitic structure. Disorder is likely to increase the pressure required to completely buckle the entire material, as observed experimentally in 45 GPa required to buckle 38% boron-doped graphite[9] compared to 35 GPa predicted for ordered BC_3. Also, this transformation may not have been direct, as it took place at 2200 K, and may have had to thermally overcome energy barriers.

Imposing order on boron-doped diamond could increase the achievable transition temperature by making a material composed of building blocks that are structures calculated to have a higher than average T_c in Fig. 1. The observation that order can increase T_c through a density of state enhancement has been made in a prior study of disorder in boron-doped diamond.[15] There are experimental reports of ordered boron-carbon graphitic structures with the stoichiometries BC_3 (Ref. 31) and BC_5.[37] BC_3, in particular, has been widely studied by theorists and there are two proposals[36,38] for making ordered diamond structures from ordered BC_3. Even if such proposals do become experimentally viable, it may still be beneficial to utilize boron concentration as a tunable parameter in the search for higher-T_c superconductors.

V. CONCLUSIONS

There is significant experimental evidence to support the possibility that boron can be inserted into diamond in a dominantly substitutional position without compensation at concentrations greater than the 5% currently achieved. Within this class of materials, we predict using a simple structural model of disorder a continuous increase of the bulk superconducting transition temperature as a function of boron concentration up to a maximum of 55 K near 30% boron. Superconductivity may persist up to even higher temperatures by percolating through regions of above-average electron-phonon coupling due to the highly inhomogeneous nature of electron-phonon coupling in this disordered material. This predicted maximum of T_c far exceeds the current highest value, $T_c=11$ K, in boron-doped diamond and even the highest value, $T_c=40$ K, of the current best conventional electron-phonon superconductor,[39] MgB_2. These results are not converged with respect to supercell size for boron concentrations larger than 25% and additional unaccounted for phonon softening may increase T_c in an intermediate doping regime before causing enough lattice distortion to open up an insulating gap and quench superconductivity at large enough doping. A more conclusive result will require further experimental input and more extensive theoretical modeling.

The limit of T_c in boron-doped diamond is also relevant to the more general question of T_c limits in conventional electron-phonon superconductors at ambient pressure. A simple model of electron-phonon coupling based only on electronic and atomic densities of a material[40] gives a value of 90 meV for $\sqrt{\lambda\langle\omega^2\rangle}$ of diamond, which is a very good estimate of the largest obtainable value in boron-doped diamond shown in Fig. 2. In this simple model, electron-phonon coupling increases monotonically with electronic density.

Simple models of bulk modulus also show a monotonic increase with electronic density,[41] and for the class of materials where both these simple models apply, the hardest material, diamond, should also have the largest electron-phonon coupling. Superconductivity has been recently reported in another doped hard semiconductor, silicon carbide.[42] Based on this scaling, other hard materials such as boron nitride, boron carbide, or carbon clathrates should also have similarly large electron-phonon coupling and have been theoretically considered for superconductivity.[43,44] It is not likely possible to significantly increase a material's electronic or atomic density at ambient pressure beyond the value in diamond, and any further increases in $\lambda\langle\omega^2\rangle$ must come from effects beyond a simple two-parameter model. Only electrons very near the Fermi level contribute to superconductivity, and by using narrow bands, reduced dimensionality, or a carefully engineered band structure, one might focus electronic states with a strong electron-phonon coupling toward the Fermi level with a resulting large $N(\epsilon_F)$ and large $\lambda\langle\omega^2\rangle$. Also considering mass factors in Eq. (4), $\lambda\langle\omega^2\rangle$ may be increased by incorporating hydrogen into a material,[45] but the lower valence of hydrogen compared to carbon might offset the mass enhancement with a reduction in the magnitude of electron-phonon matrix elements from what is calculated for diamond. Materials with large values of $\lambda\langle\omega^2\rangle$ are not enough to achieve higher T_c values; λ must also be increased by uniformly driving the phonon modes responsible for electron-phonon coupling toward instability.[11,46] The practical limitation on T_c is presently the material synthesis technology—the potential increase in T_c in going from MgB_2 to heavily boron-doped diamond requires going from a thermodynamically stable binary compound to one that might only be accessible using a multistep nonequilibrium process.

ACKNOWLEDGMENTS

This work was supported by the National Science Foundation Grant No. DMR07-05941 and by the Director, Office of Science, Office of Basic Energy Sciences, Division of Materials Sciences and Engineering Division, U.S. Department of Energy under Contract No. DE-AC02-05CH11231. Calculations in this work have been done using the QUANTUM-ESPRESSO package.[18]

*jmoussa@civet.berkeley.edu

[1] K. J. Chang, M. M. Dacorogna, M. L. Cohen, J. M. Mignot, G. Chouteau, and G. Martinez, Phys. Rev. Lett. **54**, 2375 (1985).
[2] D. A. Papaconstantopoulos, W. E. Pickett, B. M. Klein, and L. L. Boyer, Nature (London) **308**, 494 (1984).
[3] H. Rosner, A. Kitaigorodsky, and W. E. Pickett, Phys. Rev. Lett. **88**, 127001 (2002).
[4] D. A. Papaconstantopoulos and W. E. Pickett, Phys. Rev. B **31**, 7093 (1985).
[5] A. M. Fogg, J. Meldrum, G. R. Darling, J. B. Claridge, and M. J. Rosseinsky, J. Am. Chem. Soc. **128**, 10043 (2006).
[6] E. A. Ekimov, V. A. Sidorov, E. D. Bauer, N. N. Mel'nik, N. J. Curro, J. D. Thompson, and S. M. Stishov, Nature (London) **428**, 542 (2004).
[7] Y. Takano, T. Takenouchi, S. Ishii, S. Ueda, T. Okutsu, I. Sakaguchi, H. Umezawa, H. Kawarada, and M. Tachiki, Diamond Relat. Mater. **16**, 911 (2007).
[8] H. Mukuda, T. Tsuchida, A. Harada, Y. Kitaoka, T. Takenouchi, Y. Takano, M. Nagao, I. Sakaguchi, T. Oguchi, and H. Kawarada, Phys. Rev. B **75**, 033301 (2007).
[9] P. V. Zinin, L. C. Ming, I. Kudryashov, N. Konishi, N. H. Manghnani, and S. K. Sharma, J. Appl. Phys. **100**, 013516 (2006).
[10] J. K. Dewhurst, S. Sharma, C. Ambrosch-Draxl, and B. Johansson, Phys. Rev. B **68**, 020504(R) (2003).
[11] J. E. Moussa and M. L. Cohen, Phys. Rev. B **74**, 094520 (2006).
[12] H. J. Choi, D. Roundy, H. Sun, M. L. Cohen, and S. G. Louie, Phys. Rev. B **66**, 020513(R) (2002).
[13] F. Giustino, M. L. Cohen, and S. G. Louie, Phys. Rev. B **76**, 165108 (2007).
[14] K.-W. Lee and W. E. Pickett, Phys. Rev. B **73**, 075105 (2006).
[15] T. Shirakawa, S. Horiuchi, Y. Ohta, and H. Fukuyama, J. Phys. Soc. Jpn. **76**, 014711 (2007).
[16] P. W. Anderson, J. Phys. Chem. Solids **11**, 26 (1959).
[17] P. B. Allen and B. Mitrović, Solid State Phys. **37**, 2 (1982).
[18] S. Baroni, A. Dal Corso, S. de Gironcoli, P. Giannozzi, C. Cavazzoni, G. Ballabio, S. Scandolo, G. Chiarotti, P. Focher, A. Pasquarello, K. Laasonen, A. Trave, R. Car, N. Marzari, and A. Kokalj, http://www.pwscf.org/
[19] J. M. Soler, E. Artacho, J. D. Gale, A. Garca, J. Junquera, P. Ordejón, and D. Sánchez-Portal, J. Phys.: Condens. Matter **14**, 2745 (2002).
[20] K.-W. Lee and W. E. Pickett, Phys. Rev. Lett. **93**, 237003 (2004).
[21] P. B. Allen and R. C. Dynes, Phys. Rev. B **12**, 905 (1975).
[22] P. W. Anderson, K. A. Muttalib, and T. V. Ramakrishnan, Phys. Rev. B **28**, 117 (1983).
[23] T. Yokoya, T. Nakamura, T. Matsushita, T. Muro, Y. Takano, M. Nagao, T. Takenouchi, H. Kawarada, and T. Oguchi, Nature (London) **438**, 647 (2005).
[24] E. Bourgeois, E. Bustarret, P. Achatz, F. Omnès, and X. Blase, Phys. Rev. B **74**, 094509 (2006).
[25] J. P. Goss and P. R. Briddon, Phys. Rev. B **73**, 085204 (2006).
[26] J. P. Goss, P. R. Briddon, R. Jones, Z. Teukam, D. Ballutaud, F. Jomard, J. Chevallier, M. Bernard, and A. Deneuville, Phys. Rev. B **68**, 235209 (2003).
[27] R. Magri, Phys. Rev. B **49**, 2805 (1994).
[28] L. Vegard, Z. Phys. **5**, 17 (1921); Z. Kristallogr. **67**, 239 (1928).
[29] W. L. McMillan, Phys. Rev. **167**, 331 (1968).
[30] V. L. Solozhenko, N. A. Dubrovinskaia, and L. S. Dubrovinsky, Appl. Phys. Lett. **85**, 1508 (2004).
[31] J. Kouvetakis, R. B. Kaner, M. L. Sattler, and N. Bartlett, J. Chem. Soc., Chem. Commun. **1986**, 1758.
[32] T. Shirasaki, A. Derré, M. Ménétrier, A. Tressaud, and S. Flandrois, Carbon **38**, 1461 (2000).
[33] V. L. Solozhenko, O. O. Kurakevych, E. G. Solozhenko, J. Chen, and J. B. Parise, Solid State Commun. **137**, 268 (2006).
[34] V. L. Solozhenko and O. O. Kurakevych, Acta Crystallogr., Sect.

B: Struct. Sci. **61**, 498 (2005).
[35] S. Fahy, S. G. Louie, and M. L. Cohen, Phys. Rev. B **34**, 1191 (1986).
[36] Z. Jin-Ling, C. Tian, M. Yan-Ming, L. Zhi-Ming, L. Bing-Bing, and Z. Guang-Tian, Chin. Phys. Lett. **23**, 2538 (2006).
[37] B. M. Way, J. R. Dahn, T. Tiedje, K. Myrtle, and M. Kasrai, Phys. Rev. B **46**, 1697 (1992).
[38] Z. Liu, J. He, J. Yang, X. Guo, H. Sun, H.-T. Wang, E. Wu, and Y. Tian, Phys. Rev. B **73**, 172101 (2006).
[39] J. Nagamatsu, N. Nakagawa, T. Muranaka, Y. Zenitani, and J. Akimitsu, Nature (London) **410**, 63 (2001).
[40] P. K. Lam and M. L. Cohen, Phys. Lett. **97A**, 114 (1983). Note that there is a typographical error in Eq. (6); the exponent of the electron density is supposed to be 1.2.
[41] M. L. Cohen, Phys. Rev. B **32**, 7988 (1985).
[42] Z.-A. Ren, J. Kato, T. Muranaka, J. Akimitsu, M. Kriener, and Y. Maeno, J. Phys. Soc. Jpn. **76**, 103710 (2007).
[43] M. Calandra, N. Vast, and F. Mauri, Phys. Rev. B **69**, 224505 (2004).
[44] F. Zipoli, M. Bernasconi, and G. Benedek, Phys. Rev. B **74**, 205408 (2006).
[45] N. W. Ashcroft, Phys. Rev. Lett. **92**, 187002 (2004).
[46] W. E. Pickett, J. Supercond. **19**, 291 (2006).